A Journal of the Gesellschaft Deutscher Chemiker

Angewandte Chemie

International Edition

www.angewandte.org

Title: Closing the loop for hydrogen storage: Facile regeneration of NaBH4 from its hydrolytic product

Authors: Yongyang Zhu, Liuzhang Ouyang, Hao Zhong, Jiangwen Liu, Hui Wang, Huaiyu Shao, Zhenguo Huang, and Min Zhu

To be cited as: *Angew. Chem. Int. Ed.* 10.1002/anie.201915988
Angew. Chem. 10.1002/ange.201915988

Link to VoR: http://dx.doi.org/10.1002/anie.201915988
http://dx.doi.org/10.1002/ange.201915988

WILEY-VCH

Closing the loop for hydrogen storage: Facile regeneration of $NaBH_4$ from its hydrolytic product

Yongyang Zhu,[a] Liuzhang Ouyang,*[a, b] Hao Zhong,[a] Jiangwen Liu,[a] Hui Wang,[a] Huaiyu Shao,*[c] Zhenguo Huang,*[d] and Min Zhu[a]

[a] Y. Zhu, Prof. L. Ouyang, Dr. H. Zhong, Prof. J. Liu, Prof. H. Wang, Prof. M. Zhu
School of Materials Science and Engineering, Guangdong Provincial Key Laboratory of Advanced Energy Storage Materials
South China University of Technology
Guangzhou, 510641, People's Republic of China
E-mail: meouyang@scut.edu.cn
[b] Prof. L. Ouyang
China-Australia Joint Laboratory for Energy & Environmental Materials
Key Laboratory of Fuel Cell Technology of Guangdong Province
Guangzhou, 510641, People's Republic of China
[c] Prof. H. Shao
Joint Key Laboratory of the Ministry of Education, Institute of Applied Physics and Materials Engineering (IAPME), Department of Physics and Chemistry, Faculty of Science and Technology
University of Macau
Macau SAR, China
E-mail: hshao@um.edu.mo
[d] Prof. Z. Huang
School of Civil and Environmental Engineering
University of Technology Sydney
Sydney, NSW, 2007, Australia
E-mail: zhenguo.huang@uts.edu.au

Supporting information for this article is given via a link at the end of the document.

Abstract: Sodium borohydride ($NaBH_4$) is among the most studied hydrogen storage materials since it is able to deliver high purity H_2 at room temperature with controllable kinetics via hydrolysis, but its regeneration from the hydrolytic product has been challenging. Herein we report a facile method to regenerate $NaBH_4$ with high yield and low costs. The hydrolytic product $NaBO_2$ in aqueous solution reacts with CO_2 forming $Na_2B_4O_7{\cdot}10H_2O$ and Na_2CO_3, both of which are ball milled with Mg under ambient conditions to form $NaBH_4$ with a high yield close to 80 %. Compared with previous studies, this new approach avoids expensive reducing agent such as MgH_2, bypasses the energy-intensive dehydration procedure to remove water from $Na_2B_4O_7{\cdot}10H_2O$, and does not require high-pressure H_2 gas, therefore leading to much reduced costs. This method is expected to effectively close the loop of $NaBH_4$ regeneration and hydrolysis, enabling a wide deployment of $NaBH_4$ for hydrogen storage.

Introduction

Hydrogen has been deemed as an ideal energy carrier due to its high energy density by weight, high abundance, and environmental friendliness.[1] However, wide utilization of hydrogen energy has been hampered by a few barriers with one of them associated with storage. Due to its low energy density by volume, hydrogen has been conventionally compressed or liquefied to improve the density. However, these physical processes cause large energy penalty and special care is always required when operating under high pressure or cryogenic conditions. Materials-based hydrogen storage has therefore received strong attention since it has attractive features such as higher capacity, better safety, and milder operation conditions.

Sodium borohydride ($NaBH_4$) is among the most studied candidates as a hydrogen storage material. $NaBH_4$ can release hydrogen via hydrolysis with good controllability, high hydrogen purity, high gravimetric hydrogen storage capacity and environmentally benign by-products.[2] The hydrolysis of $NaBH_4$ is typically expressed by the following reaction:

$$NaBH_4 + (2+x)H_2O \rightarrow NaBO_2 \cdot xH_2O + 4H_2 \quad (1)$$

The spent fuel is normally hydrated sodium metaborate ($NaBO_2{\cdot}xH_2O$).[3] The regeneration of $NaBH_4$ from the hydrolytic product so far has featured high costs and low yields.

$NaBO_2$ in aqueous solution reacts with CO_2 in air forming $Na_2B_4O_7{\cdot}10H_2O$ and $NaCO_3$ according to the following reaction:

$$4NaBO_2{\cdot}xH_2O + CO_2 + (10-4x)\,H_2O \rightarrow Na_2B_4O_7{\cdot}10H_2O + Na_2CO_3 \quad (2)$$

$Na_2B_4O_7{\cdot}10H_2O$ is the main constituent of naturally abundant borax mineral. It is therefore highly appealing to develop a simple, efficient and affordable approach to generate $NaBH_4$ from $Na_2B_4O_7{\cdot}10H_2O$.

Currently, two types of raw materials, H_2 (H°) and metal hydride (H^-) have been used as hydrogen sources in the (re)generation of $NaBH_4$. For example, $NaBH_4$ can be synthesized by annealing $Na_2B_4O_7$ with Na and SiO_2 under high pressure H_2 (over 3 MPa) at elevated temperature (400–500°C).[4] This method is of high cost because the reaction conditions are harsh and a considerable amount of sodium metal is needed. Recently, the preparation of $NaBH_4$ has been carried out by annealing the dehydrated borax ($Na_2B_4O_7$) with low-cost magnesium (Mg) at a high temperature (550°C) and high H_2

10.1002/anie.201915988

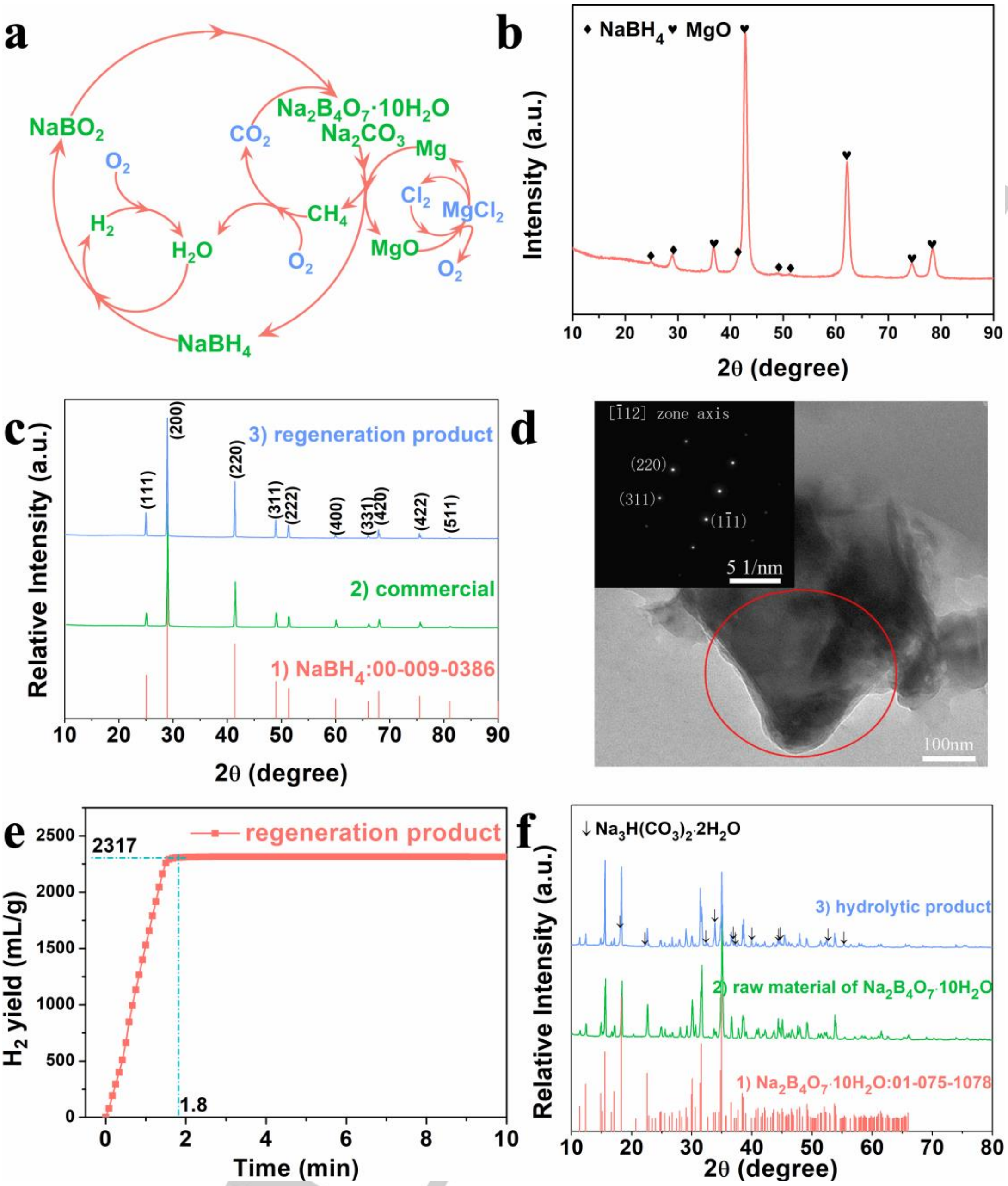

Figure 1. (a) A closed system of $NaBH_4$ hydrolysis and regeneration; (b) XRD pattern of products obtained via ball milling a mixture of Mg, $Na_2B_4O_7·10H_2O$, and Na_2CO_3 in 24.75:1:1 molar ratio for 20 h at 1000 CPM; (c) XRD patterns of standard PDF card of $NaBH_4$, commercial and synthesized $NaBH_4$; (d) TEM image and SAED pattern of synthesized $NaBH_4$; (e) Hydrolysis curve of the regenerated $NaBH_4$ in an aqueous solution loaded with 2 wt% $CoCl_2$; (f) XRD patterns of standard PDF card of $Na_2B_4O_7·10H_2O$, raw $Na_2B_4O_7·10H_2O$, and compounds obtained after hydrolytic aqueous solution naturally dried up in air.

pressure (2.5MPa).[5] However, this process is also energy intensive and dangerous. The process can be further optimized by ball milling $Na_2B_4O_7$ [6] and $NaBO_2$ [7] with magnesium hydrides (MgH_2) with a maximum yield of 78% and 76%, respectively. The use of expensive MgH_2, however, makes mass production by these methods less feasible. It should also note that high energy is required to obtain $Na_2B_4O_7$ by dehydrating $Na_2B_4O_7·10H_2O$ at approximately 600°C and $NaBO_2·xH_2O$ at temperatures over 350°C, respectively.[8] The hydrolytic by-product of $NaBH_4$ can exist in the form of $NaBO_2·xH_2O$ (x=2, 4), from a $NaBO_2$ aqueous solution via drying treatment of < 110°C.[8b] Researchers tried ball milling $NaBO_2·xH_2O$ (x=2, 4) with Mg-based alloys (e.g. Mg_2Si, Mg-Al alloy) with/without Mg at room temperature under Argon atmosphere.[9] The yield can be above 74%, but Mg-containing alloys are more expensive than Mg and more by-products (stable metal oxides for example) are formed during ball milling.[9] Therefore, Mg instead of alloys should be used as a reducing agent.

Herein, we present a new method where H^+ in the coordinate water in $Na_2B_4O_7·xH_2O$ (x=5, 10) can be directly used as a

10.1002/anie.201915988

hydrogen source to prepare $NaBH_4$. In the new procedure, a mixture of $Na_2B_4O_7 \cdot xH_2O$ (x=5, 10) and Na_2CO_3 is obtained by exposing $NaBO_2$ aqueous solution to CO_2 and then drying at a temperature of < 54°C. Ball milling the mixture with Mg at room temperature and under atmospheric pressure Argon leads to the formation of $NaBH_4$ with a high yield of 78.9%. Compared with the literature procedures (Table S1) that require dehydrated $Na_2B_4O_7/NaBO_2$, MgH_2, high pressure H_2, and/or high temperatures, this new method utilizes low-cost materials and operates under mild reaction conditions, which allows for facile scalable manufacturing and ultimately closes the loop of $NaBH_4$ regeneration and hydrolysis.

Results and Discussion

Regeneration and hydrolysis cycle

One key challenge in utilizing $NaBH_4$ for hydrogen storage lies in its regeneration. Herein we developed a facile procedure to regenerate $NaBH_4$ from its CO_2 treated hydrolytic product (Figure 1a). $NaBH_4$ can be successfully synthesized by ball milling a mixture of Mg, $Na_2B_4O_7 \cdot 10H_2O$, and Na_2CO_3 at ambient condition. Figure 1b shows XRD qualitative analysis of the powders after 20h milling of a mixture of Mg, $Na_2B_4O_7 \cdot 10H_2O$, and Na_2CO_3 in a mole ratio of 24.75:1:1. The diffraction peaks are indexed to $NaBH_4$ and MgO.

$NaBH_4$ was isolated from the as-milled product, and its identity and morphology were studied using XRD, FTIR, NMR, SEM, and TEM. XRD pattern of commercial $NaBH_4$ (Figure 1c(2)) show ten peaks at 25.1°, 28.9°, 41.4°, 49.0°, 51.3°, 60.0°, 66.0°, 68.0°, 75.5°, and 81.0°, corresponding to (111), (200), (220), (311), (222), (400), (331), (420), (422), and (511) of $NaBH_4$ (ICDD 00-009-0386), respectively. The synthesized $NaBH_4$ displays the same XRD pattern as the commercial $NaBH_4$ (Figure 1c(3)). The FTIR bands of 2200-2400 and 1125 cm^{-1} correspond to the B-H stretching and deformation of pure $NaBH_4$, respectively[10], in good agreement with the those of commercial $NaBH_4$ (Figure S2a). The XRD and FTIR results are also consistent with the previous studies on $NaBH_4$ synthesis.[7a, 9c, 10c, 11] The BH_4^- anion is further confirmed by NMR analysis (Figure S2b).[12] Similar to commercial $NaBH_4$, the synthesized $NaBH_4$ exists in cubic particles with sizes of several microns (Figure S3). Selected area electron diffraction (SAED) pattern also indicates the success in obtaining crystalline $NaBH_4$ (Figure 1d and Figure S4).

According to the results obtained from various techniques (XRD, FTIR, NMR, SEM, and TEM), we can conclude that high quality $NaBH_4$ with crystallography and microstructure similar to commercial $NaBH_4$ was successfully synthesized by directly ball milling $Na_2B_4O_7 \cdot 10H_2O$ and Na_2CO_3 with Mg in Ar at room temperature. The synthesis conditions are very mild compared with the previous studies in which $NaBH_4$ was produced via $NaBO_2$ reacting with Mg at 350°C under 7 MPa H_2[13] or $Na_2B_4O_7$ reacting with Mg at 550°C under 2.5 MPa H_2.[5]

For a closed-loop application, hydrogen evolution performance of the regenerated $NaBH_4$ is particularly important. Figure 1e shows the hydrogen production curve of prepared $NaBH_4$, which showed rapid hydrolytic H_2 evolution that produced 2317 mL/g H_2 in 1.8 min. After the hydrolytic aqueous solution was naturally dried up in air, solid $Na_2B_4O_7 \cdot 10H_2O$ (ICDD ref. 01-075-1078) powers were obtained, as evidenced by XRD patterns (Figure 1f) and FTIR spectra (Figure S5). Another set of characteristic diffraction peaks can be indexed to $Na_3H(CO_3)_2 \cdot 2H_2O$ which is composed of Na_2CO_3 and $NaHCO_3$. The transformation of Na_2CO_3 into $NaHCO_3$ occurs in the following reaction:

$$Na_2CO_3\ (aq) + CO_2 + H_2O \rightarrow 2NaHCO_3 \quad (3)$$

$NaHCO_3$ can be avoided by regulating the exposure of the hydrolytic aqueous solution to air. This is supported by experiments that only $Na_2B_4O_7 \cdot 10H_2O$ and Na_2CO_3 can be obtained by tuning the exposure of $NaBO_2$ aqueous solution to CO_2 (Figure S6).

We illustrate a pathway to close the cycle of $NaBH_4$ hydrolysis and regeneration (Figure 1a). Comparing with the literature methods, current procedure features low-cost starting materials, mild reactions at room temperature, and requiring no high pressure H_2. The energy efficiency of regeneration can be estimated by systematic modeling, which is beyond the scope of the current work. One important step in the complete cycle is the reformation of Mg metal. Although electrochemical process of extracting Mg is energy intensive, it is widely adopted industrially. The direct use of hydrated sodium tetraborate avoids an energy intensive process of drying $Na_2B_4O_7 \cdot xH_2O$ at over 600°C to obtain $Na_2B_4O_7$. In addition, by directly using the hydrate, H^+ in $Na_2B_4O_7 \cdot xH_2O$ serves as a hydrogen source for $NaBH_4$ regeneration, without the need of any external H_2 source. This process therefore reduces costs and energy consumption associated with hydrogen production. Apart from H_2, another commonly used hydrogen source in the literature is MgH_2.[6-7] This hydride is fabricated by a high-temperature (over 300°C) reaction between Mg and H_2, and H_2 is produced by a separate process. Therefore, the current work presents a promising cycle pathway for large-scale application of $NaBH_4$ as a hydrogen carrier.

Reaction mechanism

To understand the reaction, $Na_2B_4O_7 \cdot 10H_2O$, Na_2CO_3, and Mg mixtures were ball milled for relatively short periods. The XRD diffraction peaks of $Na_2B_4O_7 \cdot 10H_2O$ become invisible after 5 min milling, along with the appearance of diffraction peaks of $Na_2B_4O_7 \cdot 5H_2O$ (Figure 2a), in agreement with FTIR results (Figure 2b(2) and Figure S7). The actual formula of $Na_2B_4O_7 \cdot 5H_2O$ and $Na_2B_4O_7 \cdot 10H_2O$ are $Na_2B_4O_5(OH)_4 \cdot 3H_2O$ and $Na_2B_4O_5(OH)_4 \cdot 8H_2O$, respectively, according to the chemical structures.[14] Hydrogen can be detected in this period from the MS of the gas atmosphere (Figure S8). After 10 min of ball milling, the intensity of diffraction peaks of $Na_2B_4O_7 \cdot 5H_2O$ decreases significantly. As the milling increases to 30 min, XRD diffraction peaks of MgO become highly visible while those of $Na_2B_4O_7 \cdot 5H_2O$ and Na_2CO_3 almost disappear. Although the diffraction peaks of $NaBH_4$ are invisible, the B-H group can be detected by FTIR (Figure 2b(4)). The absorption bands of BO_3^{3-} (1500-1300 cm^{-1}) and BO_4^{5-} (1150-950 cm^{-1}) originally present in $[B_4O_5(OH)_4]^{2-}$, and of CO_3^{2-} (1450-1400 cm^{-1}, 877 cm^{-1}) originally present in Na_2CO_3 become very weak and then vanish completely from the spectra (Figure 2b). As the milling time reaches 5 h, the (200) diffraction peak of $NaBH_4$ appears.

Considering the observation of $Na_2B_4O_7 \cdot 5H_2O$ and H_2 after 5 min, the first step of the reaction is assumed as follows:

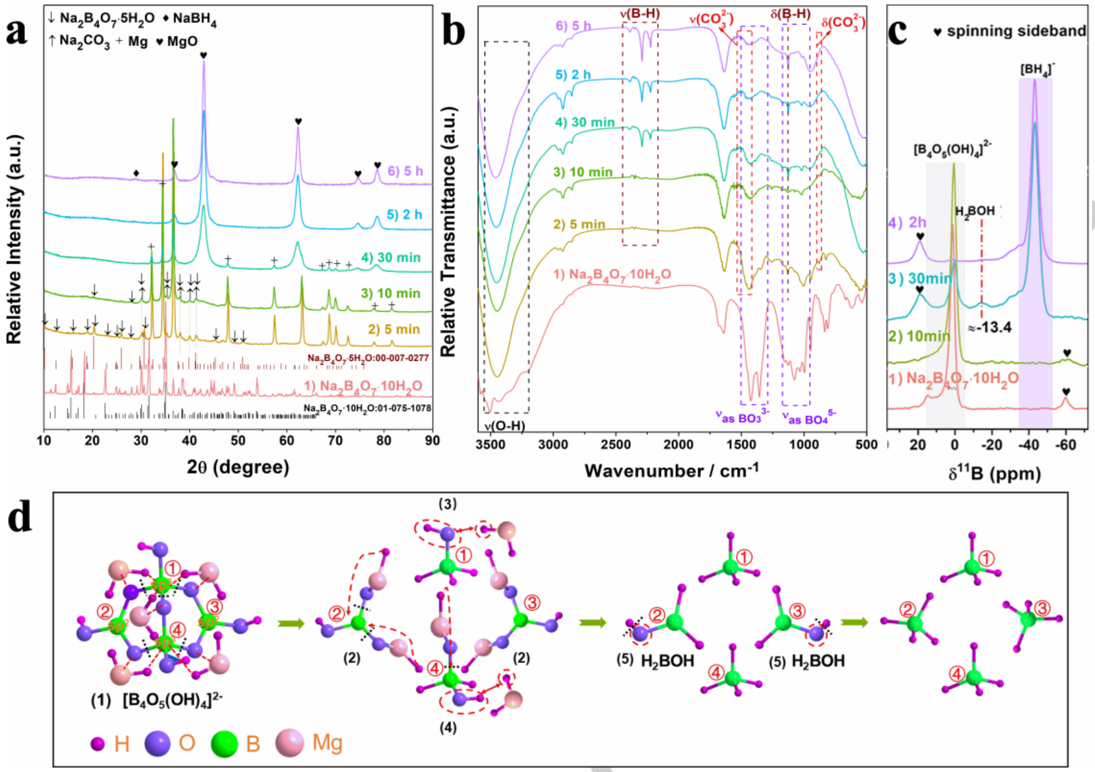

Figure 2. (a) XRD patterns and (b) FTIR spectra of commercial $Na_2B_4O_7\cdot10H_2O$ and products obtained after ball milling Mg, $Na_2B_4O_7\cdot10H_2O$, and Na_2CO_3 mixtures (in 18:1:1 molar ratio) at 1200 CPM for different durations; (c) Solid-state ^{11}B NMR spectra of commercial $Na_2B_4O_7\cdot10H_2O$ and products obtained after ball milling for different durations; (d) Proposed reaction mechanism between Mg, Na_2CO_3, and $Na_2B_4O_7\cdot10H_2O$ to form $NaBH_4$.

$$Na_2B_4O_7\cdot10H_2O \rightarrow Na_2B_4O_7\cdot5H_2O + 5H_2O \quad (4)$$

$$2H_2O + Mg \rightarrow Mg(OH)_2 + H_2 \quad (5)$$

Under the experiment conditions, the following reactions will subsequently occur as large amounts of magnesium still exist: [10b, 15]

$$Mg + Mg(OH)_2 \rightarrow 2MgO + H_2 \quad (6)$$

$$H_2 + Mg \rightarrow MgH_2 \quad (7)$$

With increasing milling time, $NaBH_4$, MgO, and also CH_4 (Figure S8 and Figure S9) were observed which is associated with this reaction:

$$Na_2B_4O_7\cdot5H_2O + Na_2CO_3 + 15MgH_2 \rightarrow 4NaBH_4 + 15MgO + CH_4 + 10H_2 \quad (8)$$

The overall reaction equation is therefore can be expressed in the following equation:

$$Na_2B_4O_7\cdot10H_2O + Na_2CO_3 + 20Mg \rightarrow 4NaBH_4 + 20MgO + CH_4 \quad (9)$$

This reaction is calculated to be favourable in thermodynamics (ΔG^o_{298k}= -1326.18 kJ/mol of $NaBH_4$).

In this closed-loop regeneration (Figure 1a), CH_4 can be collected and converted to CO_2, which is then used to produce Na_2CO_3. Mg can be regenerated via the commercial method, where MgO is first converted to $MgCl_2$ and Mg is obtained by electrolysis of $MgCl_2$.

MgH_2 was not observed in this study, probably because it was consumed *in-situ* due to its high activity. This is in agreement with a previous study where MgH_2 was proposed as an intermediate during $NaBH_4$ regeneration via ball milling $NaB(OH)_4$ and Mg.[10b] It should be noted that MgH_2 could form via a reaction between Mg and H_2 in the presence of oxide and hydroxide species. Unlike dense Al_2O_3, MgO or $Mg(OH)_2$ layer is relative loose so H_2 can penetrate through to react with underlying Mg. In addition, during ball milling, oxide and hydroxide layers on Mg will be destroyed and fresh Mg surfaces are always produced. Based upon thermodynamic calculation (Table S2), MgO is more stable than MgH_2 (ΔG^o_r of MgO: -565.95 kJ/mol, ΔG^o_r of MgH_2: -35.09 kJ/mol). In this work, MgH_2 formed in reaction (7) is highly reductive, converting $Na_2B_4O_7$ to $NaBH_4$ and forming stable MgO in the end.

The formation of methane is likely due to the reaction between Na_2CO_3 and MgH_2.[16] H_2 was not in the overall reaction (eqn 9) but was observed by MS, which is due to the nature of gas-solid reaction between H_2 and Mg, where it is hard to achieve 100 % conversion.

To further elucidate the reaction mechanism, the ball milled products were characterized by solid-state ^{11}B magic-angle spinning (MAS) NMR (Figure 2c). After 10 min of ball milling, only $[B_4O_5(OH)_4]^{2-}$ is detected (Figure 2c(2)). The resonance observed at ≈-13.4 ppm in Figure 2c(3) after 30 min milling demonstrates the formation of intermediate H_2BOH.[11, 17] The reaction transformation of $[B_4O_5(OH)_4]^{2-}$ is therefore proposed as shown in Figure 2d. The unit of $[B_4O_5(OH)_4]^{2-}$ contains two BO_4 tetrahedra and two BO_3 triangles as showed in Figure 2d(1). The B-O bond (average bond length: 1.3683 Å) in BO_3 triangles is stronger

10.1002/anie.201915988

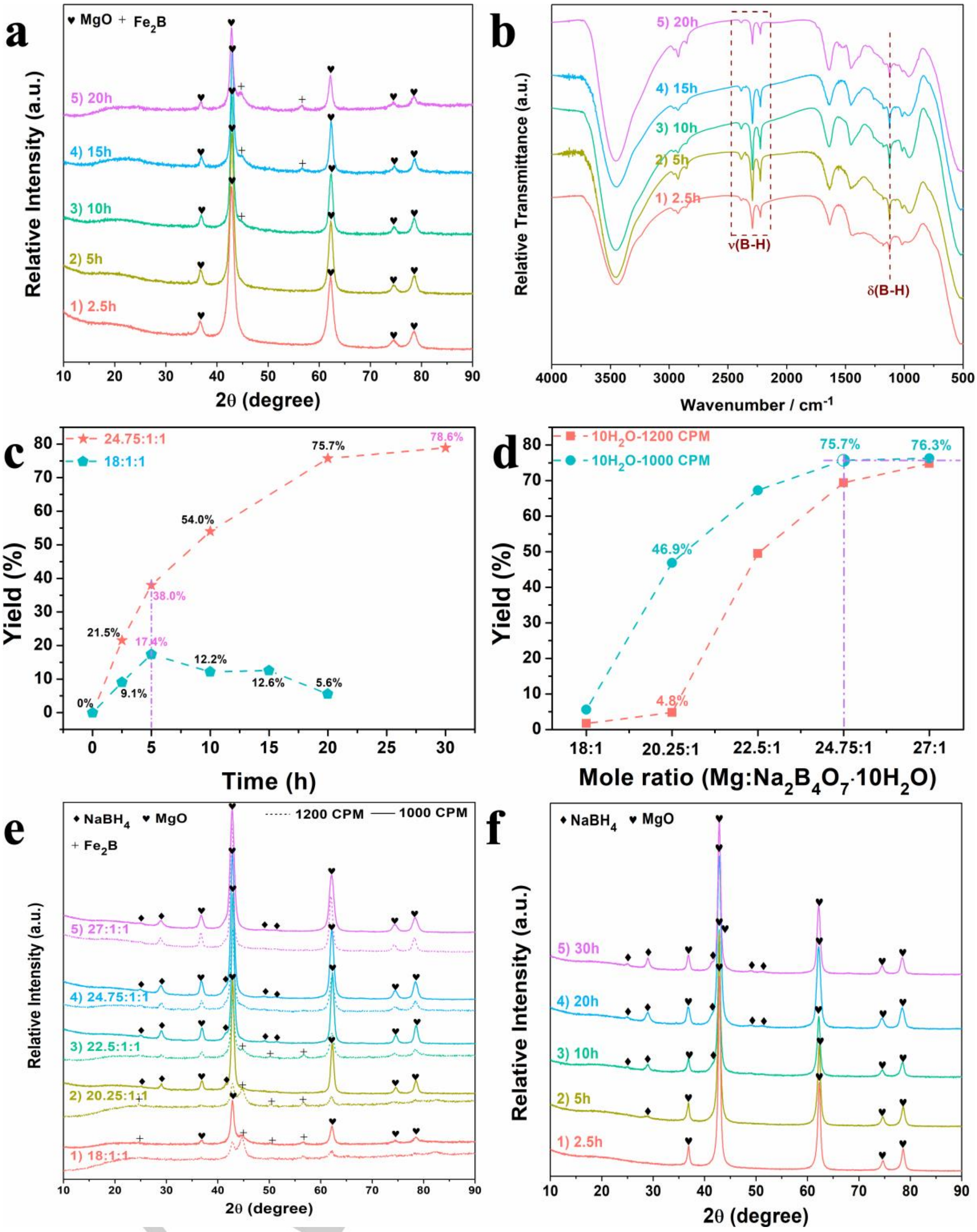

Figure 3. (a) XRD patterns and (b) FTIR spectra of the products obtained after ball milling Mg, $Na_2B_4O_7\cdot10H_2O$, and Na_2CO_3 mixtures (in 18:1:1 molar ratio) at 1000 CPM for different durations; (c) Yields of $NaBH_4$ with reactants in different molar ratios at 1000 CPM for different durations; (d) Yields of $NaBH_4$ and (e) XRD patterns of the products obtained after ball milling Mg and $Na_2B_4O_7\cdot10H_2O$ in different molar ratios ($Na_2B_4O_7\cdot10H_2O$ and Na_2CO_3 were fixed at 1:1 molar ratio) for 20h at 1000 CPM and 1200 CPM, respectively; (f) XRD patterns of the products obtained via ball milling Mg, $Na_2B_4O_7\cdot10H_2O$, and Na_2CO_3 in a molar ratio of 24.75:1:1 at 1000 CPM for different durations.

than the one (average bond length: 1.4418 Å) in BO_4 tetrahedra.[18] Thus, the B-O in BO_4 tetrahedra preferentially breaks, and B forms bond with the H in MgH_2 and the O forms bond with Mg. It is reasonable to assume that three intermediates are formed (Figure 2d(2-4)). Thermodynamically, Mg is more likely to bond with oxygen to form a more stable compound, MgO

(ΔG_f^o of MgO: -569.3 kJ/mol oxygen; ΔG_f^o of B_2O_3: -398.1 kJ/mol oxygen).[19] Therefore, B-O and Mg-H in the B-O-Mg-H intermediate break and the B-H and MgO are formed (Figure 2d(2,4)). The breaking of the (B)-O-H (O bonded with sp^2 boron) in Figure 2d(5) results into formation of intermediate "H_2BOH", which is detected in NMR spectra (Figure 2c(3)). According to the literature, [11] B in "H_2BOH" is Lewis acidic and could accept H^- from MgH_2. As a result, "BH_4^-" and MgO are generated. In addition, "OH^-" bonded with sp^3 boron (Figure 2d(3,4)) is substituted by H^- in MgH_2 forming "BH_4^-", which agrees with previous studies.[10b]

Yield of $NaBH_4$

Efforts have been made to optimize the yield of $NaBH_4$ by ball milling CO_2 treated hydrolytic products (a mixture of $Na_2B_4O_7{\cdot}10H_2O$ and Na_2CO_3) with Mg. Figure 3a shows the XRD patterns of the products obtained by ball milling Mg, $Na_2B_4O_7{\cdot}10H_2O$, and Na_2CO_3 in a 18:1:1 molar ratio for different durations. After 2.5 h of ball milling, the diffraction peaks of starting materials disappear, along with the appearance of strong diffraction peaks of MgO. Although the diffraction peaks of $NaBH_4$ are invisible, the typical B-H bands (2200-2400 and 1125 cm^{-1}) are detectable by FTIR (Figure 3b(1)), which indicates the formation of $NaBH_4$ after 2.5h ball milling. As milling time increases to 10h, the diffraction peaks assigned to Fe_2B become visible (Figure 3a(3)). With further increase in milling time, the diffraction peaks of Fe_2B become stronger while the characteristic FTIR bands of $NaBH_4$ become weaker. The FTIR results indicate that the yield of $NaBH_4$ firstly increases and then decreases with the milling time (Figure 3b). Iodometric analysis was carried to quantify $NaBH_4$ after its isolation from the ball-milled product. The relationship between the yield and milling time is consistent with FTIR results (Figure 3b, c), reflecting the fact that $NaBH_4$ was decomposed after long-time ball-milling. This is likely due to the reaction between $NaBH_4$ and Fe (peeling off the balls and jar after long-time ball-milling), as evidenced by the formation of more Fe_2B as milling time increases (Figure 3a). The highest yield among the five durations for the mixture with 18:1:1 molar ratio is about 17.4% after 5 h of ball milling (Figure 3c).

The impact of Mg loading on the yield was also studied (Figure 3d). For 20h milling, the yield increased when more Mg was used, and it was ~46.9% for a molar ratio of 20.25:1:1 (Mg: $Na_2B_4O_7{\cdot}10H_2O$: Na_2CO_3), and reached the maximum of 75.7% for a ratio of 24.75:1:1. The highest yield of 78.9% was obtained after 30 h of ball milling for the sample with 24.75:1:1 mole ratio (Figure 3c), which is higher than the $NaBO_2{\cdot}2H_2O$-Mg system reported previously (68.55%, Table S1).[10b] There are a few possible reasons for this improvement in yield. Firstly, from the calculation, reaction (9) is thermodynamically more favorable than reaction (10) due to its larger ΔG^o_r value (Table S3). Secondly, Na_2CO_3 in $Na_2B_4O_7{\cdot}10H_2O$-Na_2CO_3-Mg system may work as a dispersant to prevent the materials (especially Mg) sticking onto the walls of the jar and balls, resulting in better ball-milling efficiency and favorable yield. Thirdly, comparing to $NaBO_2$, $Na_2B_4O_7$ has a higher reactivity for recycling to $NaBH_4$.[3b] Lastly, the speed of 1000 CPM leads to better yield than 1200 CPM, the reason of which will be discussed later.[10b] For this particular batch, the yield after 5 h (38.0%) is already much higher than that with 18:1:1, and the XRD diffraction peaks of $NaBH_4$ are clearly visible (Figure 3f). Yields can be improved by increasing the amount of Mg used, which is consistent with previous studies. [6-7, 19-20] With a high loading of Mg, powders do not stick to the jar and balls, resulting in better the ball-milling efficiency. In addition, more Mg leads to better contact among all the reactants resulting in favorable yield. Limited by the ball mill machine, only two milling speeds, 1000 and 1200 CPM, were tried, which proves that ball mill speed, i.e. energy, does impact the yield. Although the energy is higher at 1200 CPM, we fail to obtain better yields under any circumstances, especially for a low molar ratio (Figure 3d). This is because more Fe peels off the balls and jar for small amount of Mg at high speed and promotes $NaBH_4$ decomposition (Figure 3e).

We have also found that when $Na_2B_4O_7{\cdot}10H_2O$ and $Na_2B_4O_7{\cdot}5H_2O$ were ball milled simultaneously with Na_2CO_3 and Mg in a molar ratio of 0.6:0.4:1:22, $NaBH_4$ was also successfully synthesized (Figure S10). Mg can also be replaced by Al or Ca to synthesize $NaBH_4$ (Figure S11). More research is needed to optimize the yields of $NaBH_4$ from these reactions.

Conclusion

In summary, we present a closed pathway for utilizing $NaBH_4$ for hydrogen storage. The regeneration of $NaBH_4$ can be achieved by ball milling its CO_2 treated hydrolytic product ($Na_2B_4O_7{\cdot}10H_2O$ and Na_2CO_3) and Mg under ambient condition, with the yield being among the highest reported so far. This process outperforms the literature methods in several key aspects. First of all, the current yield is the best among the reported literatures [5-6, 7, 10b, 13, 21] (Table S1). Secondly, the direct use of $Na_2B_4O_7{\cdot}10H_2O$ avoids high temperatures (over 600°C [8a]) required to dehydrate $Na_2B_4O_7{\cdot}10H_2O$. Thirdly, this process does not need expensive MgH_2, which is usually obtained by high-temperature reaction between Mg and H_2. When comparing this method with reported process using MgH_2, Na_2CO_3 and $Na_2B_4O_7$,[6a] the cost of the raw materials in this method is reduced by 24-fold (Table S4). This indicates a promising pathway for large-scale application of $NaBH_4$ as a hydrogen carrier.

Acknowledgements

This work was financially supported by the National Key R&D Program of China (No. 2018YFB15-02100), Foundation for Innovative Research Groups of the National Natural Science Foundation of China (No. NSFC51621001), National Natural Science Foundation of China Projects (No. 51771075) and Natural Science Foundation of Guangdong Province of China (2016A030312011). Z.H. acknowledges support under the Australian Research Council's Discovery Projects funding scheme (project number DP170101773). Shao acknowledges support from Macau Science and Technology Development Fund (FDCT) (Project No.: 0062/2018/A2 and 118/2016/A3).

Keywords: borohydride • hydrolysis • hydrogen • hydrogen storage • regeneration

[1] a) A. F. Dalebrook, W. Gan, M. Grasemann, S. Moret, G. Laurenczy, *Chem. Commun.* **2013**, *49*, 8735-8751; b) I. P. Jain, *Int. J. Hydrogen Energy* **2009**, *34*, 7368-7378; c) L. Schlapbach, A. Züttel, *Nature* **2001**, *414*, 353-358.

[2] a) Y. Kojima, Y. Kawai, H. Nakanishi, S. Matsumoto, *J. Power Sources* **2004**, *135*, 36-41; b) R. B. Biniwale, S. Rayalu, S. Devotta, M. Ichikawa, *Int. J. Hydrogen Energy* **2008**, *33*, 360-365; c) E. Y. Marreroalfonso, A. M. Beaird, T. A. Davis, M. A. Matthews, *Ind. Eng. Chem. Res.* **2009**, *48*, 3703-3712..

[3] a) M. A. Budroni, S. Garroni, G. R. C. Mulas, M. Rustici, *J. Phys. Chem. C* **2017**, *121*, 4891-4898; b) E. H. Park, S. U. Jeong, U. H. Jung, S. H. Kim, J. Lee, S. W. Nam, T. H. Lim, Y. J. Park, Y. H. Yu, *Int. J. Hydrogen Energy* **2007**, *32*, 2982-2987.

[4] F. Schubert, K. Lang, W. Schlabacher, DE Pat. 1067005, **1959**.

[5] İ. Kayacan, Ö. M. Doğan, B. Z. Uysal, *Int. J. Hydrogen Energy* **2011**, *36*, 7410-7415.

[6] a) Z. P. Li, N. Morigazaki, B. H. Liu, S. Suda, *J. Alloys Compd.* **2003**, *349*, 232-236; b) C. Çakanyıldırım, M. Gürü, *Energy Sources* **2012**, *34*, 1104-1113.

[7] a) C. L. Hsueh, C. H. Liu, B. H. Chen, C. Y. Chen, Y. C. Kuo, K. J. Hwang, J. R. Ku, *Int. J. Hydrogen Energy* **2009**, *34*, 1717-1725; b) L. Kong, X. Cui, H. Jin, J. Wu, H. Du, T. Xiong, *Energy Fuels* **2009**, *23*, 5049-5054; c) W. Chen, L. Z. Ouyang, J. W. Liu, X. D. Yao, H. Wang, Z. W. Liu, M. Zhu, *J. Power Sources* **2017**, *359*, 400-407.

[8] a) A. Ekmekyapar, A. Ahmet Baysar, A. Künkül, *Ind. Eng. Chem. Res.* **1997**, *36*, 3487-3490; b) A. M. Beaird, P. Li, H. S. Marsh, W. Al-Saidi, J. K. Johnson, M. A. Matthews, C. T. Williams, *Ind. Eng. Chem. Res.* **2011**, *50*, 7746-7752.

[9] a) T. T. Le, C. Pistidda, J. Puszkiel, C. Milanese, S. Garroni, T. Emmler, G. Capurso, G. Gizer, T. Klassen, M. Dornheim, *Metals* **2019**, 9, 1061; b) H. Zhong, L. Z. Ouyang, J. W. Liu, C. H. Peng, X. K. Zhu, W. H. Zhu, F. Fang, M. Zhu, *J. Power Sources* **2018**, *390*, 71-77; c) M. J. Huang, H. Zhong, L. Z. Ouyang, C. H. Peng, X. K. Zhu, W. H. Zhu, F. Fang, M. Zhu, *J. Alloys Compd.* **2017**, *729*, 1079-1085.

[10] a) L. Z. Ouyang, H. Zhong, Z. M. Li, Z. J. Cao, H. Wang, J. W. Liu, X. K. Zhu, M. Zhu, *J. Power Sources* **2014**, *269*, 768-772; b) L. Ouyang, W. Chen, J. Liu, M. Felderhoff, H. Wang, M. Zhu, *Adv. Energy Mater.* **2017**, *7*, 1700299; c) H. Zhong, L. Z. Ouyang, J. S. Ye, J. W. Liu, H. Wang, X. D. Yao, M. Zhu, *Energy Storage Materials* **2017**, *7*, 222-228.

[11] C. Lang, Y. Jia, J. Liu, H. Wang, L. Ouyang, M. Zhu, X. Yao, *Int. J. Hydrogen Energy* **2017**, *42*, 13127-13135.

[12] J. Huang, Y. Yan, A. Remhof, Y. Zhang, D. Rentsch, Y. S. Au, P. E. D. Jongh, F. Cuevas, L. Ouyang, M. Zhu, *Dalton Trans.* **2016**, *45*, 3687-3690.

[13] Y. Kojima, T. Haga, *Int. J. Hydrogen Energy* **2003**, *28*, 989-993.

[14] I. Waclawska, *J. Therm. Anal.* **1995**, *43*, 261-269.

[15] P. Tessier, E. Akiba, *J. Alloys Compd.* **1999**, *293-295*, 400-402.

[16] a) E. Mukhina, A. Kolesnikov, V. Kutcherov, *Scientific reports* **2017**, *7*, 5749; b) J. Y. Chen, L. J. Jin, J. P. Dong, H. F. Zheng, G. Y. Liu, *Chin. Chem. Lett.* **2008**, *19*, 475-478.

[17] A. C. Stowe, W. J. Shaw, J. C. Linehan, B. Schmid, T. Autrey, *Phys. Chem. Chem. Phys.* **2007**, *9*, 1831-1836.

[18] Y. Wang, S. Pan, X. Hou, L. Gang, D. Jia, *Solid State Sci.* **2015**, *42*, 1726-1730.

[19] Z. P. Li, B. H. Liu, N. Morigasaki, S. Suda, *J. Alloys Compd.* **2003**, *354*, 243-247.

[20] Ç. Çakanyıldırım, M. Gürü, *Renewable Energy* **2010**, *35*, 1895-1899.

[21] a) Ç. Çakanyildirim, M. Gürü, *Energy Sources, Part A Recovery, Util. Environ. Eff.* **2011** 33, 1912-1920; b) B. H. Liu, Z. P. Li, J. K. Zhu, *J. Alloys Compd.* **2009**, *476*, L16-L20.

10.1002/anie.201915988

Entry for the Table of Contents

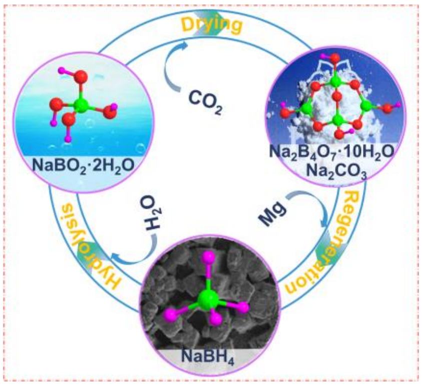

We report a facile method to regenerate $NaBH_4$ with high yield and low cost from its hydrolytic product $NaBO_2$. This method expects to effectively close the loop of $NaBH_4$ hydrolysis and regeneration and therefore enables a wide deployment of $NaBH_4$ for hydrogen storage.

Yongyang Zhu, Liuzhang Ouyang, Hao Zhong, Jiangwen Liu, Hui Wang, Huaiyu Shao*, Zhenguo Huang*, and Min Zhu*

Closing the loop for hydrogen storage: Facile regeneration of $NaBH_4$ from its hydrolytic product